**P7.2** Scale-dependent dynamic models for LES: Surface heterogeneity effects

Rob Stoll* and Fernando Porté-Agel
Saint Anthony Falls Laboratory
University of Minnesota, Minneapolis, Minnesota

## 1. Introduction

The study of surface heterogeneity effects on atmospheric boundary layer (ABL) dynamics requires detailed knowledge of the turbulence at a wide range of spatial and temporal scales. Large-eddy simulation (LES) can provide this kind of information. LES consists of explicitly solving the unsteady three-dimensional equations governing turbulent transport for all scales larger than the grid size $\Delta_{LES}$ while the effect of the sub-grid scales (smaller than $\Delta_{LES}$) on the resolved scales is parameterized. The separation of scales is achieved by spatially filtering the governing equations for momentum and scalar transport at a scale $\Delta \geq \Delta_{LES}$. The sub-grid scale (SGS) quantities that must be modeled in LES are the SGS stresses $\tau_{ij}$ and SGS fluxes $q_i$, defined as

$$\tau_{ij} = \widetilde{u_i u_j} - \tilde{u_i}\tilde{u_j} \quad \text{and} \tag{1}$$

$$q_i = \widetilde{u_i \theta} - \tilde{u_i}\tilde{\theta}, \tag{2}$$

respectively. The ($\tilde{}$) represents the LES filtering operation, $u_i$ is the velocity in the $i$-direction and $\theta$ is a generic scalar quantity.

The SGS stresses and SGS fluxes must be parameterized using information available in the resolved (filtered) velocity and scalar fields. This is one of the major challenges in LES due to the sensitivity of simulation results to both the model formulation and the way in which the model coefficient(s) are specified (Meneveau and Katz, 2000). In heterogeneous flows, the model coefficients are expected to depend on local flow characteristics (e.g. local shear stress and atmospheric stability). This dependence needs to be accounted for in order to improve the accuracy of LES in simulations of heterogeneous ABLs. In this paper, we develop and implement a new SGS model that does not require any parameter specification or tuning since the model coefficient is computed dynamically at every position in the flow and time step based on the resolved field. The model is based on using the Lagrangian averaging technique introduced by Meneveau et al (1996) in the framework of the scale-dependent dynamic model developed by Porté-Agel et al (2000) for the SGS stresses and Porté-Agel (2004) for the SGS scalar fluxes. This modification is essential in simulations of ABLs over heterogeneous surfaces, where the flow is not homogeneous over horizontal planes (as typically assumed in dynamic models). The model is tested in simulations of both homogeneous and heterogeneous ABLs.

*Corresponding author address: R. Stoll, Saint Anthony Falls, 2 3rd Avenue SE, Minneapolis, MN 55414, e-mail: stolli@msi.umn.edu

## 2. Model Formulation

The proposed scale-dependent Lagrangian dynamic model uses the Lagrangian averaging technique developed by Meneveau et al (1996) to allow a consistent application of the scale-dependent dynamic model, introduced by Porté-Agel et al (2000) for the SGS stresses and Porté-Agel (2004) for the SGS fluxes, to heterogeneous flows. The base models are an eddy-viscosity model for the deviatoric part of $\tau_{ij}$ and an eddy-diffusion model for $q_i$:

$$\tau_{ij} - \frac{1}{3}\delta_{ij}\tau_{kk} = -2(\Delta C_s)^2 |\tilde{S}|\tilde{S}_{ij} \tag{3}$$

$$q_i = -\Delta^2 C_s^2 Sc^{-1} |\tilde{S}| \frac{\partial \tilde{\theta}}{\partial x_i}. \tag{4}$$

In Eqs. 3 and 4, $\tilde{S}_{ij} = 1/2(\partial\tilde{u}_i/\partial x_j + \partial\tilde{u}_j/\partial x_i)$ is the resolved strain rate tensor with magnitude $|\tilde{S}| = 2(\tilde{S}_{ij}\tilde{S}_{ij})^{1/2}$, $C_s$ is the Smagorinsky coefficient, and $C_s^2 Sc^{-1}$ is a lumped coefficient that comprises $C_s$ and the SGS Schmidt/Prandtl number ($Sc$).

Next, a brief description of the scale-dependent dynamic procedure applied to the calculation of $C_s$ is given. More details can be found in Porté-Agel et al (2000) for the SGS stresses and Porté-Agel (2004) for the SGS fluxes. The model is based on the Germano identity (Germano et al, 1991)

$$L_{ij} = \overline{\tilde{u}_i \tilde{u}_j} - \bar{\tilde{u}}_i \bar{\tilde{u}}_j = T_{ij} - \bar{\tau}_{ij}, \tag{5}$$

where $L_{ij}$ is a resolved stress tensor and $T_{ij}$ is the SGS stress at the test-filter scale $\bar{\Delta}(= 2\Delta$ here). $T_{ij}$ can be computed using the eddy-viscosity model as

$$T_{ij} - \frac{1}{3}\delta_{ij}T_{kk} = -2[2\Delta C_s(2\Delta)]^2 |\bar{\tilde{S}}|\bar{\tilde{S}}_{ij}. \tag{6}$$

Substituting Eq. 6 and Eq. 3 into Eq. 5 results in the following system of equations:

$$L_{ij} = C_s^2(\Delta) M_{ij} \ , \tag{7}$$

where

$$M_{ij} = 2\Delta^2 \left( \overline{|\tilde{S}|\tilde{S}_{ij}} - 4\beta |\bar{\tilde{S}}|\bar{\tilde{S}}_{ij} \right). \tag{8}$$

Minimizing the error in Eq. 7 and averaging over directions of statistical homogeneity (Ghosal et al, 1995) or fluid pathlines (Meneveau et al, 1996) gives

$$C_s^2(\Delta) = \frac{\langle L_{ij} M_{ij} \rangle}{\langle M_{ij} M_{ij} \rangle} \tag{9}$$

where $\langle\ \rangle$ denotes an averaging operator and $M_{ij}$ contains the scale-dependent parameter $\beta = C_s^2(2\Delta)/C_s^2(\Delta)$. In order to dynamically calculate $\beta$, the same dynamic procedure is used with a second test filter ($\hat{}$) applied at another test-filter scale

$\widehat{\Delta} = 4\Delta$ in the Germano identity (Eq. 5). This results in a second equation for $C_s^2(\Delta)$

$$C_s^2(\Delta) = \frac{\left\langle L'_{ij} M'_{ij} \right\rangle}{\left\langle M'_{ij} M'_{ij} \right\rangle} \tag{10}$$

where

$$L'_{ij} = \widehat{\tilde{u}_i \tilde{u}_j} - \hat{\tilde{u}}_i \hat{\tilde{u}}_j \text{ and} \tag{11}$$

$$M'_{ij} = 2\Delta^2 \left( \widehat{|\tilde{S}|\tilde{S}_{ij}} - 4^2 \beta^2 |\hat{\tilde{S}}| \hat{\tilde{S}}_{ij} \right). \tag{12}$$

In Eq. 12 the assumption is made that $C_s^2(2\Delta)/C_s^2(\Delta) = C_s^2(4\Delta)/C_s^2(2\Delta)$ and therefore $C_s^2(4\Delta)/C_s^2(\Delta) = \beta^2$. By combining Eqs. 9 and 10 one obtains an equation from which the single unknown parameter $\beta$ can be computed,

$$\langle L_{ij} M_{ij} \rangle \left\langle M'_{ij} M'_{ij} \right\rangle - \left\langle L'_{ij} M'_{ij} \right\rangle \langle M_{ij} M_{ij} \rangle = 0. \tag{13}$$

The value of $\beta$ from Eq. 13 is then used in Eq. 9 to find the Smagorinsky coefficient $C_s$.

In previous studies, the scale-dependent dynamic model (Porté-Agel et al, 2000; Porté-Agel, 2004), was applied in horizontally homogeneous ABL flows. Therefore, averaging over horizontal planes was used as the natural choice in Eqs. 9 and 13. Here, in order to use the dynamic model over heterogeneous surfaces, we apply instead the Lagrangian averaging procedure developed by Meneveau et al (1996). This procedure involves solving a relaxation transport equation for each term ($L_{ij}M_{ij}$, $M_{ij}M_{ij}$, $L'_{ij}M'_{ij}$ and $M'_{ij}M'_{ij}$) along fluid pathlines. With the assumption of an exponential relaxation function and a first order discretization in time, the Lagrangian averages for $L_{ij}M_{ij}$ and $M_{ij}M_{ij}$ are:

$$\oint_{LM}^{n+1}(\boldsymbol{x}) = H\{\epsilon \left[L_{ij}M_{ij}\right]^{n+1} + (1-\epsilon)\oint_{LM}^{n}(\boldsymbol{x} - \boldsymbol{u}^n \Delta t)\} \tag{14}$$

and

$$\oint_{MM}^{n+1}(\boldsymbol{x}) = \epsilon \left[M_{ij}M_{ij}\right]^{n+1} + (1-\epsilon)\oint_{MM}^{n}(\boldsymbol{x} - \boldsymbol{u}^n \Delta t), \tag{15}$$

where

$$\epsilon \equiv \frac{\Delta t / T_{2\Delta}^n}{1 + \Delta t / T_{2\Delta}^n}, \text{ with } T_{2\Delta}^n = 1.5\Delta \left( \oint_{LM}^n \oint_{MM}^n \right)^{-1/8}. \tag{16}$$

In Eq. 14 $H\{x\}$ is a ramp function [$H\{x\} = x,\ x \geq 0; H\{x\} = 0,\ x < 0$] and the position $\boldsymbol{x} - \boldsymbol{u}^n \Delta t$ at the previous time step is calculated using multilinear interpolation. The Lagrangian averages for $L'_{ij}M'_{ij}$ and $M'_{ij}M'_{ij}$ are found in an equivalent manner to Eqs. 14 and 15, respectively, with the appropriate timescale $T_{4\Delta}^n = 1.5\Delta \left( \oint_{L'M'}^n \oint_{M'M'}^n \right)^{-1/8}$. The Lagrangian averaged model coefficient $C_s^2(\boldsymbol{x}, t)$ and scale-dependent parameter $\beta(\boldsymbol{x}, t)$ at each time step and every position in the flow, are now found from

$$C_s^2(\boldsymbol{x}, t) = \frac{\oint_{LM}}{\oint_{MM}}, \text{ and} \tag{17}$$

$$\oint_{LM} \oint_{M'M'} - \oint_{L'M'} \oint_{MM} = 0. \tag{18}$$

The Lagrangian averaged lumped coefficient $C_s^2 Sc^{-1}(\boldsymbol{x}, t)$ and scale-dependence parameter $\beta_\theta(\boldsymbol{x}, t) = C_s^2 Sc^{-1}(2\Delta)/C_s^2 Sc^{-1}(\Delta)$ for the eddy-diffusion model (Eq. 4) are computed in the same manner as for the eddy-viscosity model, i.e.,

$$C_s^2 Sc^{-1}(\boldsymbol{x}, t) = \frac{\oint_{KX}}{\oint_{XX}} \tag{19}$$

$$\oint_{KX} \oint_{X'X'} - \oint_{K'X'} \oint_{XX} = 0. \tag{20}$$

In Eqs. 19 and 20, the Lagrangian averages are the equivalent forms of Eqs. 14 and 15 with, for example, $K_i$ replacing $L_{ij}$ and $X_i$ replacing $M_{ij}$, where

$$K_i = \overline{\tilde{u}_i \tilde{\theta}} - \bar{\tilde{u}}_i \bar{\tilde{\theta}} \tag{21}$$

$$X_i = \Delta^2 \left( \overline{|\tilde{S}| \frac{\partial \tilde{\theta}}{\partial x_i}} - 4\beta_\theta \left| \bar{\tilde{S}} \right| \frac{\partial \bar{\tilde{\theta}}}{\partial x_i} \right). \tag{22}$$

In Eq. 22, the assumption is also made that $C_s^2 Sc^{-1}(2\Delta)/C_s^2 Sc^{-1}(\Delta) = C_s^2 Sc^{-1}(4\Delta)/C_s^2 Sc^{-1}(2\Delta) = \beta_\theta$. Also note that the dimensionally appropriate relaxation time scale for eddy-diffusion (for the first test filter) is $T_{2\Delta}^n = 1.5\sigma_\theta \Delta (\oint_{KX} \oint_{XX})^{-1/4}$, where $\sigma_\theta$ is the standard deviation of the resolved scalar concentration.

In the next section, the scale-dependent Lagrangian dynamic models for the SGS stress and the SGS flux are implemented in LES of the ABL over both homogeneous and heterogeneous surface conditions.

## 3. Numerical Simulations

The scale-dependent Lagrangian dynamic model is implemented in a modified version of the LES code described by Porté-Agel et al (2000) and Porté-Agel (2004). The size of the simulation domain is $L_x$ x $L_y$ x $L_z$, where $L_z = H = 1000$ m ($H$ is the boundary layer height) and $L_x = L_y = 2\pi L_z$. The domain is divided into 54 x 54 x 54 grid points for the homogeneous case and 80 x 80 x 80 grid points for the heterogeneous case. Boundary conditions in the horizontal directions are periodic. The top boundary condition is a zero-flux condition and the bottom (surface) boundary condition is given by Monin-Obukhov similarity.

### 3.1 *Homogeneous Case: Model Verification*

First, we present results from a homogeneous neutral (no buoyancy effects) ABL with a constant surface flux of a passive scalar. These results are compared with similarity theory for the mean profiles of the vertical streamwise velocity gradient and vertical scalar gradient. Streamwise velocity spectra are also presented and compared with the well-known spectral scaling for a neutral, high-Reynolds-number boundary layer.

Figure 1 shows the averaged non-dimensional streamwise velocity gradient $\Phi = \kappa z u_*^{-1} dU/dz$ ($\kappa = 0.4$ is the von Kármán constant and $u_*$ is the friction velocity) obtained with simulations using the scale-dependent Lagrangian dynamic model over a homogeneous surface under neutral conditions. $\Phi$ is plotted versus the normalized height z/H. Similarity theory predicts that $\Phi$ will have a constant value of one in the surface layer (approximately the lower 10% of the boundary layer) (Businger et al, 1971) and a slightly larger value in the wake layer

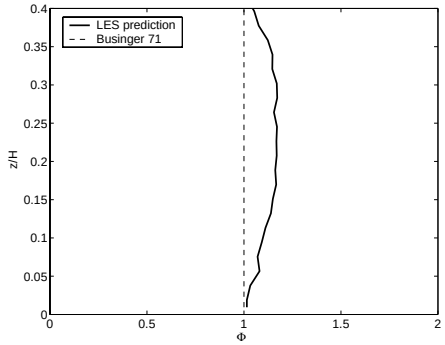


FIG. 1: Non-dimensional vertical gradient of the mean streamwise velocity $\Phi = \frac{\kappa z}{u_*}\frac{dU}{dz}$ from a simulation of a neutral ABL. The dashed line corresponds to the classical log-law (expected to hold throughout the surface layer - approximately the lower 10% of the ABL) with $\kappa = 0.4$.

above. As seen in figure 1 the model reproduces this behavior for $\Phi$ in the lower part of the boundary layer.

The non-dimensional vertical scalar concentration gradient $\Phi_\theta = \frac{\kappa z}{\theta_*}\frac{d\langle\tilde{\theta}\rangle}{dz}$ is shown in figure 2 as a function of z/H. Here, $\theta_* = q_w u_*^{-1}$, where $q_w$ is the scalar surface flux. For the passive scalar concentration, $\Phi_\theta$ is expected to have a constant value of 0.74 in the surface layer (Businger et al, 1971). The non-dimensional gradient in figure 2 is fairly constant and close to the empirical value in the surface layer. As expected, its value is larger in the wake region.

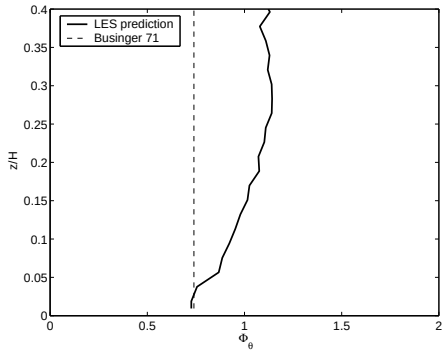


FIG. 2: Non-dimensional vertical gradient of the mean scalar concentration $\Phi_\theta = \frac{\kappa z}{\theta_*}\frac{d\langle\tilde{\theta}\rangle}{dz}$ from a simulation of a neutral ABL with a constant passive scalar surface flux. The dashed line corresponds to the classical log-law (expected to hold throughout the surface layer) with $\kappa = 0.4$.

Next, we explore how the model reproduces the distribution of the simulated kinetic energy as a function of scale by analyzing the streamwise velocity spectra computed at different heights in the boundary layer. In a neutrally stable ABL, properly normalized (as in figure 3) streamwise velocity spectra are expected to collapse and scale as $k_1^{-5/3}$ in the inertial subrange (wavenumbers $k_1 \geq z^{-1}$, where $k_1$ is streamwise wavenumber and $z$ is height). For smaller wavenumbers ($H^{-1} \leq k_1 \leq z^{-1}$), corresponding to the production subrange, spectra are expected to scale as $k_1^{-1}$, with a change from $k_1^{-1}$ to $k_1^{-5/3}$ scaling taking place near $k_1 z = 1$ (Perry et al, 1986). This scaling behavior is well reproduced by the spectra shown in figure 3.

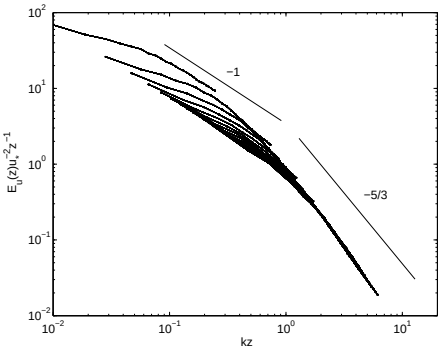


FIG. 3: Normalized streamwise velocity spectra at different heights from homogeneous neutral simulations with the scale-dependent Lagrangian dynamic model.

### 3.2 *Heterogeneous Test Case*

To demonstrate the ability of the new SGS models to capture the spatial distribution of the dynamically computed coefficients and scale-dependent parameters, a simulation was run over a surface with a simple heterogeneous distribution of both passive scalar flux $q_w$ and aerodynamic surface roughness $z_o$. Half of the domain ($0 < x/H < \pi$) consists of a relatively 'rough' ($z_o = 0.25$ m) surface with positive scalar flux ($q_w^R$). The other half ($\pi < x/H < 2\pi$) is a relatively 'smooth' ($z_o = 0.025$ m) surface with negative scalar flux ($q_w^S = -q_w^R$). The transition between the two surface types is abrupt and the pattern is periodic due to the horizontal periodic boundary conditions used.

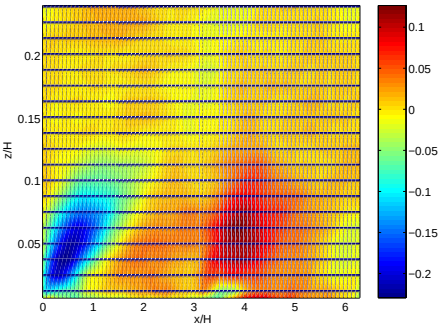


FIG. 4: Normalized deviation from the plane averaged value $(\langle C_s\rangle|_{(x,z)} - \langle C_s\rangle|_{(z)})/\langle C_s\rangle|_{(z)}$ of $C_s$ for flow over a heterogeneous surface (roughness and scalar flux change at $x/H = \pi$).

The spatial distribution of the eddy-viscosity coefficient $C_s$ and the lumped eddy-diffusion coefficient $C_s^2 Sc^{-1}$, obtained with the scale-dependent Lagrangian dynamic models over the heterogeneous surface, are presented in figures 4 and 5, respectively. Both coefficients show a strong decrease right after the smooth-to-rough transition. This adjustment is consistent with the increase in mean shear created by the sudden increase in surface roughness. Note that in Eqs. 3 and 4 the model coefficients act to modulate the characteristic

turbulence length scale in the eddy-viscosity and eddy-diffusion models. Therefore, the coefficients must decrease to account for the reduction in characteristic length scales associated with an increase in the mean shear. The opposite effect is observed after the rough-to-smooth transition at $x/H = \pi$. In this case, the mean shear decreases, allowing for the length scales of the flow to increase at a given height near the surface. This effect translates into a larger value of both coefficients. It is important to notice that the heterogeneity in the spatial distribution of $C_s^2 Sc^{-1}$ is relatively stronger and extends higher up in the ABL compared with $C_s$. This effect could not be captured by assuming a constant value of $Sc$.

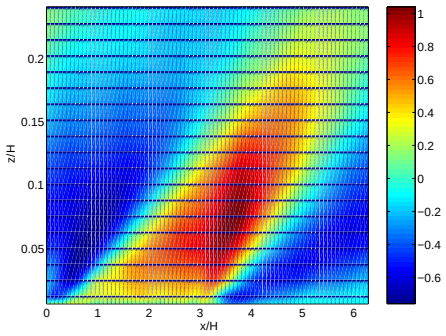


FIG. 5: Normalized deviation from the plane averaged value $(\langle C_s^2 Sc^{-1}\rangle|_{(x,z)} - \langle C_s^2 Sc^{-1}\rangle|_{(z)})/\langle C_s^2 Sc^{-1}\rangle|_{(z)}$ of $C_s^2 Sc^{-1}$ for flow over a heterogeneous surface (roughness and scalar flux change at $x/H = \pi$).

The spatial distribution of the scale-dependence parameter $\beta$ is shown in figure 6 at different streamwise positions in the flow versus the normalized height z/H. $\beta$ decreases as the flow transitions from smooth to rough and has the opposite trend after the transition from rough to smooth. These results can be understood considering that $\beta$ is directly related to the level of anisotropy of the flow at the smallest resolved scales (Porté-Agel et al, 2000; Porté-Agel, 2004). $\beta$ is expected to be much smaller than one when/where the flow becomes more anisotropic (e.g., near the surface). This is consistent with the trends observed over the heterogeneous surface and shown in figure 6. Notice that the parameter is smallest right after the smooth-to-rough transition because of the increased anisotropy associated with larger mean shear associated with the roughness change in that region. Near the center and the downwind side of both patches $\beta$ approaches a similar value near the surface.

## 4. Summary

Scale-dependent Lagrangian dynamic models for the SGS stress and SGS flux are developed and implemented in LES of both homogeneous and heterogeneous boundary layers. These models allow for parameter-free simulations as they use information in the resolved flow to provide a consistent, dynamic calculation of the model coefficients and scale-dependence parameters at every position in the flow and at each time step. In simulations of a neutral homogeneous boundary layer with a constant and uniform surface flux of a passive scalar, the models are able to give good predictions for the expected mean

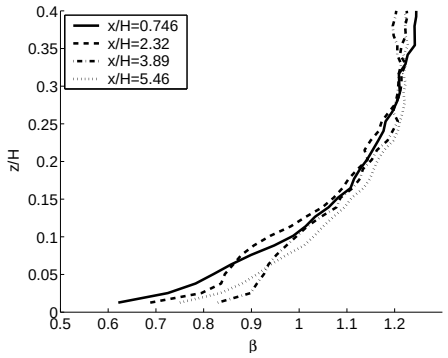


FIG. 6: Scale-dependence parameter for the eddy-viscosity model at selected streamwise positions. The height $z$ is normalized by the boundary layer height $H$.

profiles of streamwise velocity and scalar concentration (in agreement with similarity theory) as well as proper scaling of turbulent spectra. When applied to a heterogeneous boundary layer the coefficients are able to adjust in a self-consistent way to the local changes in the mean flow conditions. Future work will focus on the performance of the models under a variety of surface heterogeneity conditions (including local gradients of temperature). Furthermore, LESs with the new SGS models will be used to study the effect of different surface heterogeneity patterns on regional-scale fluxes with the ultimate goal of improving parameterizations of subgrid-scale heterogeneity in weather models.


### Acknowledgements

The authors gratefully acknowledge funding from NSF (grants EAR-0094200 and EAR-0120914 as part of the National Center for Earth-Surface Dynamics) and NASA (grants NAG5-10569 and NAG5-11801). Computing resources were provided by the University of Minnesota Supercomputing Institute.


### References


Businger, JA, Wyngaard, JC, Izumi, Y, and Bradley, EF 1971 Flux-Profile Relationships in the Atmospheric Surface Layer *J. Atmos. Sci.* **28** 181-189.

Germano, M, Piomelli, U, Moin, P and Cabot, WH 1991 A Dynamic Subgrid-Scale Eddy Viscosity Model *Phys. Fluids* **3** 1760-1765.

Ghosal, S, Lund, TS, Moin, P and Akselvoli, K 1995 A Dynamic Localization Model for Large-Eddy Simulation of Turbulent Flows *J. Fluid Mech.* **286** 229-255.

Meneveau, C and Katz, J 2000 Scale-invariance and Turbulence Models for Large-Eddy Simulation *Annu. Rev. Fluid Mech.* **32** 1-32.

Meneveau, C, Lund, TS, Cabot, WH 1996 A Lagrangian Dynamic Subgrid-Scale Model of Turbulence *J. Fluid Mech.* **319** 353-385.

Perry, AE, Henbest, SM and Chong, MS 1986 A Theoretical and Experimental Study of Wall Turbulence *J. Fluid Mech.* **165** 163-199.

Porté-Agel, F 2004 A Scale-Dependent Dynamic Model for Scalar Transport in Large-Eddy Simulations of the Atmospheric Boundary Layer *Boundary-Layer Meteorol.* **112** 81-105.

Porté-Agel, F, Meneveau, C and Parlange, MB 2000 A Scale-Dependent Dynamic Model for Large-Eddy Simulations: Application to a Neutral Atmospheric Boundary Layer *J. Fluid Mech.* **415** 261-284.